Stay-green protein, defective in Mendel's green cotyledon mutant, acts independent and upstream of pheophorbide *a* oxygenase in the chlorophyll catabolic pathway

Sylvain Aubry · Jan Mani · Stefan Hörtensteiner

Abstract Type C stay-green mutants are defined as being defective in the pathway of chlorophyll breakdown, which involves pheophorbide *a* oxygenase (PAO), required for loss of green color. By analyzing senescence parameters, such as protein degradation, expression of senescence-associated genes and loss of photosynthetic capacity, we demonstrate that JI2775, the green cotyledon (*i*) pea line used by Gregor Mendel to establish the law of genetics, is a true type C stay-green mutant. *STAY-GREEN* (*SGR*) had earlier been shown to map to the *I* locus. The defect in JI2775 is due to both reduced expression of *SGR* and loss of SGR protein function. Regulation of PAO through SGR had been proposed. By determining PAO protein abundance and activity, we show that PAO is unaffected in JI2775. Furthermore we show that pheophorbide *a* accumulation in the mutant is independent of PAO. When silencing *SGR* expression in *Arabidopsis pao1* mutant, both pheophorbide *a* accumulation and cell death phenotype, typical features of *pao1*, are lost. These results confirm that SGR function within the chlorophyll catabolic pathway is independent and upstream of PAO.

Keywords Chlorophyll breakdown · Gregor Mendel · Pea *I* locus · Pheophorbide *a* oxygenase · Stay-green mutant · Senescence

Abbreviations
chl	Chlorophyll
chlide	Chlorophyllide
EST	Expressed sequence tags
LHCII	Light harvesting complex of photosystem II
NCCs	Nonfluorescent chlorophyll catabolites
pheide	Pheophorbide
PAO	Pheophorbide *a* oxygenase
pFCC	Primary fluorescent chlorophyll catabolite
PS	Photosystem
RCCR	Red chlorophyll catabolite reductase
Sgr	Stay-green

S. Aubry · S. Hörtensteiner (✉)
Institute of Plant Biology, University of Zurich, Zollikerstrasse 107, 8008 Zurich, Switzerland
e-mail: shorten@botinst.uzh.ch

J. Mani · S. Hörtensteiner
Institute of Plant Sciences, University of Bern, Altenbergrain 21, 3013 Bern, Switzerland

Present Address:
J. Mani
Institute of Cell Biology, University of Bern, Baltzerstr. 4, 3012 Bern, Switzerland

Introduction

Chlorophyll (chl) breakdown is widely used as a tool for monitoring physiological senescence in plants. Thereby green chl is converted in a multistep pathway to linear colorless and nonfluorescent tetrapyrroles, NCCs. The pathway starts with the consecutive removal from chl of phytol and the Mg atom by chlorophyllase and a metal-chelating substance, respectively. Loss of the green color occurs during the subsequent opening of the porphyrin macrocycle of pheophorbide (pheide) *a* by the coupled action of pheide *a* oxygenase (PAO) and red chl catabolite reductase (RCCR). This yields a primary fluorescent

catabolite (pFCC), which is exported from the plastid by a primary active transporter. Further steps in the pathway are reminiscent of detoxification processes widely occurring in plants (Kreuz et al. 1996). Thus, pFCCs are activated by hydroxylation and after further modification they are imported into the vacuole by another primary active transport system. Due to the acidic vacuolar pH, FCCs eventually tautomerize non-enzymatically to NCCs (Oberhuber et al. 2003; Hörtensteiner 2006).

All but one of the NCCs isolated so far from higher plants have been shown to derive from chl *a* (Hörtensteiner 2006; Müller et al. 2006). One reason for this is the substrate-specificity of PAO for pheide *a*, with pheide *b* being a competitive inhibitor (Hörtensteiner et al. 1995). Furthermore, reduction of chl *b* to chl *a* within the chl-protein complexes of the photosystems (PS), has been suggested a prerequisite for chl degradation, leading to the destabilization of these chl-protein complexes (Hörtensteiner 2006). The recent cloning of NYC1 from rice (Kusaba et al. 2007) corroborated this assumption. *nyc1* mutants show a stay-green phenotype and besides the retention of both chl *a* and *b*, *nyc1* specifically retains light harvesting complex of photosystem II (LHCII) subunits known to bind large proportions of chl *b*. In this respect NYC1 represent an early (primary) element of metabolic regulation of chl breakdown.

Another step of regulation is at the level of PAO. Like NYC1, PAO expression is senescence-specific and absence of PAO in a respective mutant, *pao1*, leads to a stay-green phenotype in the dark. Due to the accumulation of phototoxic pheide *a*, *pao1* plants show a light-dependent lesion mimic phenotype (Pružinská et al. 2005).

Recently, a third type of stay-green mutants has become a major focus in plant senescence research. These mutants are defective in a gene identified in the Bf993 mutant of *Festuca pratensis* (Thomas 1987). The gene was termed *SID* (*senescence-induced degradation*), but orthologous genes from rice, pea and *Arabidopsis* have now been designated *SGR* (*STAY-GREEN*) (Jiang et al. 2007; Park et al. 2007; Sato et al. 2007), *SGN* (Park et al. 2007) or *NYE1* (*nonyellowing*) (Ren et al. 2007). Introgression of the *sid* locus into different *Lolium* species allowed the molecular tagging of the gene (Thomas 1997). By exploiting the high micro synteny between *Lolium-Festuca* and rice, it was possible to identify the candidate locus in a *Lolium* stay-green mapping population that corresponded to a stay-green locus (*SGR*) in rice (Armstead et al. 2006). Silencing of the orthologous gene, *AtSGR1* (At4 g22920) of *Arabidopsis*, caused the same stay-greenness as in *Festuca* or *Lolium* (Armstead et al. 2007).

Furthermore, it has been shown that *SGR* maps to the *I* locus of Mendel's green cotyledon mutant (Armstead et al. 2007). Thus, the *I* locus is only the third identified locus of

the seven traits Gregor Mendel used for establishing his laws of genetic inheritance (Mendel 1866). The first locus that has been molecularly identified is the so-called *r* (*rugosus*) locus. The mutation, which is due to a 0.8 kb insertion, resides in a gene encoding a starch branching enzyme and causes the formation of wrinkled seeds (Bhattacharyya et al. 1990). The second identified gene (*Le* locus), encodes gibberellin 3β-hydroxylase. The loss of function missense mutation near the active site abolishes gibberellin biosynthesis and, thus, affects stem length (Lester et al. 1997). Recently, the mutation of Mendel's *I* locus was elucidated molecularly (Sato et al. 2007). In contrast to an earlier finding of reduced *SGR* gene expression in the mutant (Armstead et al. 2007), gene expression was found to be normal. By complementing a rice *sgr* mutant with rice *SGR* gene exhibiting a 6-bp-insertion, it was concluded that the analogous mutation present in Mendel's green pea *SGR* gene abolished SGR function (Sato et al. 2007).

The *Festuca sid* mutant is a classical representative of the so-called 'cosmetic' type C stay-green mutants (Thomas and Howarth 2000). In these non-functional stay-greens, retention of chl is uncoupled from other senescence events, such as loss of photosynthetic capacity, which proceed normally (Hilditch et al. 1986, 1989). Hence, the gene mutations of type C mutants were considered to affect the pathway of chl breakdown directly. This has been confirmed and is obvious for *pao1* and *nyc1*, which are affected in catabolic steps of the pathway (Pružinská et al. 2003, 2005; Kusaba et al. 2007). The situation is different for *sgr/sid* mutants, since so far the function of SGR/SID could not unequivocally be demonstrated. Several early reports deal with the biochemical lesion of *sid* and *sid*-like mutants, including Mendel's *I* mutant (Vicentini et al. 1995; Thomas et al. 1996; Roca et al. 2004). The cumulative results of these investigations indicated that SGR/SID affects PAO activity. Thus, the mutants consistently accumulated chlorophyllide (chlide) and pheide *a* during senescence and they exhibited reduced PAO activities. It was argued that pheide *a* accumulation would feed back inhibit chl breakdown, in order to prevent further chl intermediate accumulation, thereby minimizing the phototoxic potential of these pigments (Thomas 1997; Matile et al. 1999; Hörtensteiner 2006). Along with the retention of chl, chl-binding proteins were shown to be retained in the mutants (Hilditch et al. 1989; Jiang et al. 2007; Park et al. 2007; Sato et al. 2007). Recently, it was demonstrated that rice SGR is able to specifically interact with LHCII subunits (Park et al. 2007). This together with the retention of these proteins in the mutants, suggested that SGR might be involved in dismantling chl-protein complexes as a prerequisite for both chl and apoprotein degradation.

The aim of this study was to thoroughly characterize Mendel's pea mutant (JI2775) in respect to senescence and

chl breakdown. We confirm that JI2775 is a classical type C stay-green mutant by analyzing different parameters of senescence, such as chl fluorescence and degradation, expression of senescence associated genes and protein degradation. We further show that JI2775 is impaired not only in SGR protein function, but by *SGR* expression and SGR immunoblot analysis demonstrate that gene expression is affected as well in the mutant. We re-addressed the proposed linkage between SGR and PAO. Using PAO activity assays and immunoblot analysis, we show that PAO function is unaffected in JI2775. Furthermore, we show that the amount of pheide *a* accumulating in the mutant is independent of the activity of PAO. Silencing of *SGR* expression in *pao1*, results in the losses of pheide *a* accumulation and cell death phenotype, typical features of *pao1*. We conclude that the function of SGR is upstream and independent of PAO. This together with the previously demonstrated interaction of SGR with LHCII, and retention during senescence of *sgr* mutants of chl binding proteins indicates a (predominant) role of SGR in dismantling of chl-protein complexes during senescence.

Experimental procedures

Plant material and senescence induction

Pisum sativum lines JI4 (yellow cotyledons) and JI2775 (green cotyledons) were obtained from the *Pisum* germplasm collection of the John Innes Center, Norwich, UK. The Columbia (Col-0) ecotype of *Arabidopsis* (*Arabidopsis thaliana*) was used as wild type. For silencing of *AtSGR1* by RNA interference, a pHannibal-derived construct as described in Armstead et al. (2007) was used. *pao1* was transformed by a floral dip method and homozygous *pao1 atsgr1*i lines selected by kanamycin resistance. This was possible, since *pao1* is not resistant to kanamycin (Alonso et al. 2003; Pružinská et al. 2005). Production of the *AtSGR1*-silencing lines, *atsgr1*i, has been described (Armstead et al. 2007). A homozygous *AtSGR2* T-DNA insertion line of the SALK collection (Alonso et al. 2003) was obtained from the European Arabidopsis Stock Center, Nottingham, UK. T-DNA insertion was verified by sequencing a PCR product obtained with the left T-DNA border primer LBb1 (5′-GCGTGGACCGCTTGCTGCAA T-3′) and an *AtSGR2*-specific primer (5′-GCAACTGGT GAAAGCAAGAAC-3′). A *Lolium* line carrying a *sid* gene introgression has been described (Roca et al. 2004) and was obtained from H. Ougham, IGER, Aberystwyth, Wales, UK.

Plants were grown on soil in long-day condition (16 h/8 h) under fluorescent light of 60–120 μmol photons $m^{-2} s^{-1}$ at 22°C. For senescence induction, leaves from 3- to 4-week-old plants were excised and incubated in permanent darkness on wet filter paper for up to 11 days at ambient temperature. Alternatively, attached leaves were individually covered with aluminum foil.

Cloning strategy

Genomic DNA and cDNA was isolated from both JI4 and JI2775 leaves as described (Murray and Thompson 1980; Pružinská et al. 2005). *PsSGR* was amplified with primers PsSGR-LP (5′-CG*GGATCC*ATGGATACTCTAACGAG TGCTC-3′) and PsSGR-RP (5′-TT*CTGCAG*TTACAAGTT ACCATGTTGGGTTC-3′) using the proofreading Pfu polymerase (Promega). After digestion with *Bam*HI and *Pst*I, fragments were cloned into pQE30 (Qiagen) to yield pQEJI4 and pQEJI2775, and inserts sequenced. For constructing binary plasmids, *SGR* open reading frames were amplified from both pQE plasmids with PsSGR-LP2 (5′-GT A*CCATGG*ATACTCTAACGAGTGCTCCTTTACTC-3′) and PsSGR-RP2 (5′-GC*GGATCC*TTACAAGTTACCATG TTGGGTTC-3′) and, after restriction with *Nco*I and *Bam*HI cloned into pHannibal (Wesley et al. 2001) containing the CaMV 35S-double enhancer promoter and a *nos* terminator. The gene constructs were excised by *Not*I and cloned into pGreen0029 (Hellens et al. 2000) yielding pGr-JI4-SGR and pGr-JI2775-SGR, respectively. After verifying inserts by sequencing, constructs were transformed into *Agrobacterium* together with pSOUP (Hellens et al. 2000).

Plant transformation

For transient expression in *Nicotiana benthamiana* leaves, 5 ml of *Agrobacterium* harboring the respective plasmids were grown overnight at 28°C. Cells were collected by centrifugation (3,000 g, 15 min), pellets resuspended in 1 ml of acetosyringone buffer (1 mM $MgCl_2$, 150 mM acetosyringone, 1 mM Mes-KOH pH 5.6) and grown again for 4 h (Llave et al. 2000). Using a 1 ml syringe, the abaxial side of leaves of 5-week-old *N. benthamiana* plants was infiltrated with the *Agrobacterium* cultures. For transformation of *Arabidopsis pao1* with a pHannibal-derived *AtSGR1* silencing construct (Armstead et al. 2007), the floral dip method was used (Sidler et al. 1998).

RNA isolation and real-time PCR

For RT-PCR analysis, total RNA was prepared from *Pisum* leaves and reverse transcribed as described (Pružinská et al. 2005). Quantitative PCR was performed in a Light-Cycler (Roche Diagnostics) using the QuantiTect SYBR Green PCR kit (Qiagen). 10- to 100-fold dilutions of first-strand cDNA reaction mixes (corresponding to 0.3–3 ng of RNA) were employed in 20 μl reactions and were used to

calculate the real-time PCR efficiency of each sample. The relative expression ratios of target gene (SGR) were calculated in comparison to a reference gene, *ACT2* (Kürsteiner et al. 2003). For semiquantitative and/or quantitative PCR the following specific primers were used: *PsACT2* (forward, 5′-TGGAATCCACGAGACAACCTA-3′ and reverse, 5′-T TCTGTGAACGATTCCTGGAC-3′); *PsSGR* (forward, 5′-ACGGTGACGGCAATTTATTC-3′ and reverse, 5′-TTCA ACGGTGGAAAACAACA-3′); *PsSAG12* (forward, 5′-TC TGAGCAAGAGCTTGTGGA-3′ and reverse 5′-TATCCCC CAGCATCAATAGC-3′); *AtSGR1* (forward, 5′-TGGGCAA ATAGGCTATACCG-3′ and reverse, 5′-AAGTTCCCATC TCCATGCAC-3′); *AtSGR2* (forward, 5′-TCCAACATCC CGGAGTAC-3′ and reverse, 5′-AGGGTTAGGTATTTCC AAC-3′); *ACT2* (forward, 5′-TGGAATCCACGAGACA ACCTA-3′ and reverse, 5′-TTCTGTGAACGATTCCTG GAC-3′).

Southern blot analysis

High molecular weight genomic DNA was isolated from both *Pisum* lines (Chakraborti et al. 2006). Each 15 μg was digested with restriction endonucleases, electrophoresed on 0.9% agarose gels and transferred to positively charged nylon membrane (Roche). The blot was hybridized overnight at 42°C with a digoxigenin-UTP-labeled 1.5 kb PCR fragment (using pQEJI4 and primers PsSGR-RP and PsSGR-LP) and washed at 65°C with 0.2× SSC, 0.1% SDS. Subsequent detection by anti-digoxigenin-AP (Roche), and bromochloroindolyl phosphate/nitroblue tetrazolium as substrate was according to the manufacturer's protocol.

Analysis of chl and chl catabolites

Chl was isolated from dark-incubated *Arabidopsis* and pea leaves, or from *N. benthamiana* according to Pružinská et al. (2005) and chl concentrations were determined spectrophotometrically (Strain et al. 1971). Chl and green pigments (chlide and pheide) were extracted and analyzed as described (Pružinská et al. 2005). For bipyridyl treatments, leaf discs were senesced in the dark by floating on water, 1% DMSO or 1 mM 2,2′-bipyridyl (containing 1% DMSO).

PAO protein extraction and activity measurement

PAO was isolated from *Pisum* chloroplast membranes by Triton X-100 solubilization according to a standard procedure (Hörtensteiner et al. 1995; Pružinská et al. 2005; Ren et al. 2007). PAO activity was monitored *in vitro* essentially as described (Pružinská et al. 2007) but using 0.06 μg μl^{-1} of His$_6$-AtRCCR (Pružinská et al. 2007), and 100 U of catalase (Sigma) to replace red chl catabolite-forming factor (Pružinská et al. 2005). pFCC formation was followed by

reversed-phase HPLC and fluorescence detection (320/450 nm) using 36% (v/v) 50 mM potassium phosphate buffer, pH 7, in methanol as solvent (Pružinská et al. 2005).

Production of anti-AtSGR antiserum and immunoblot analysis

A polyclonal anti-AtSGR antiserum was obtained from rabbits immunized with two polypeptides directed against two AtSGR peptides (NH$_2$-EGVNGYSGTQTEGIAT-COOH and NH$_2$-SQSINNSQLQGWAN-COOH). The serum was purified by affinity purification and tested by ELISA (Eurogentec, Seraing, Belgium).

After separation by SDS-PAGE, proteins were transferred to nitrocellulose membranes according to standard procedures. Proteins were labeled with monoclonal antibodies against PAO (1:500; Gray et al. 2004) and polyclonal antibodies against the following proteins: AtSGR (1:1,000), LHCII (1:2,000; Pružinská et al. 2003), Rubisco small subunit (1:2,000; S. Gepstein, Israel), Rubisco LS (1:2,000; S. Gepstein, Israel), PsaA (1:5,000; J.D. Rochaix, Geneva, Switzerland), PsaD (1:5,000; J.D. Rochaix, Geneva, Switzerland), Lhca (1:2,000; AgriSera, Sweden), PsbA (1:1,000; H. Ougham, Aberystwyth, Wales), and Cytf (1:1,000; H. Ougham, Aberystwyth, Wales). Subsequently, the membranes were labeled with alkaline phosphatase- or peroxidase-conjugated secondary antibodies, and visualized using bromochloroindolyl phosphate/nitroblue tetrazolium (PsbA and Cytf), or with the chemiluminescent peroxidase substrate kit (Sigma). Chemiluminescence signals were quantified using an ImageQuant 400 system (GE Healthcare). Immunoblot analyses were carried out in duplicate or triplicate.

Chlorophyll fluorescence and CO$_2$ assimilation rate

Senescence was induced by darkening attached leaves with aluminum foil. Using a portable photosynthesis system LI-COR 6400 (Li-Cor, Lincoln, NE), maximum quantum yield of PSII (F_v/F_m) and minimal chl *a* fluorescence following dark incubation (F_0) were determined. Quantum efficiency of electron transport through PSII (ΦPSII) was measured after adaptation to day light for 20 min (Maxwell and Johnson 2000). Rates of CO$_2$ assimilation were determined at a flux density of 500 μmol m^{-2} s^{-1} and a CO$_2$ concentration of 380 μmol mol^{-1}.

SGR protein accession numbers

The GenBank accession numbers of SGRs and SGR-like proteins in plants, algae and bacteria species are as follows: *Arabidopsis thaliana* AtSGR1, AAW82962; AtSGR2, AAU05981; AtSGR3, AAM14392; *Bacillus sp.* BsSGR1,

ZP_01859452; BsSGR2, ZP_01170511; *Clostridium botulinum* CbSGR, CAL83726; *Clostridium purfigens* CpSGR, Q8XH99; *Glycine max* GmSGR1, AAW82959; GmSGR2, AAW82960; *Hordeum vulgare* HvSGR, AAW82955; *Lycopersicon esculentum* LeSGR, AAY98500; *Oryza sativa* OsSGR1, AAW82954; OsSGR2, BAF16284; OsSGR3, CAE05787; *Ostreococcus lucimarinus* OlSGR, XP_001420948; *Ostreococcus tauri* OtSGR, CAL56489; *Pisum sativum* PsSGR-JI4, CAP04954; PsSGR-JI2775, CAP04955; *Sorghum bicolor* SbSGR, AAW82958; *Vitis vinifera* VvSGR1, CAO63641; VvSGR2, CAO63642; VvSGR3, CAN81476; *Zea mays* ZmSGR1, AAW82956; ZmSGR2, AAW82957; *Zoysia japonica* ZjSGR, AAW82961. The following protein sequences were obtained from the Joint Genome Institute (http://jgi.doe.gov) (protein IDs are given) *Populus trichocarpa* PtSGR1, 548540; PtSGR2, 646534; *Chlamydomonas reinhardtii* CrSGR1, 144728; CrSGR2, 168164; *Physcomitrella patens* PpSGR1, 128024; PpSGR2, 139487; PpSGR3, 114221; PpSGR4, 27214.

Results and discussion

Mendel's *i* mutant exhibits a non-functional stay-green phenotype

Gregor Mendel's green cotyledon mutant, JI2775 (*i/i*), was compared with JI4 (*I/I*), a wild type line showing normal yellowing of seeds during maturation (Fig. 1a) (White 1916). JI4 and JI2775 are non-isogenic lines and exhibit some differences in respect to morphology, like a difference in average size of mature leaves (JI4: 12.63 ± 1.24 cm^2; JI2775: 8.33 ± 1.25 cm^2), or seed weight (JI4: 284 ± 30.5 mg; JI2775: 212.25 ± 39 mg). The stay-green phenotype of JI2775 was evident in all green parts of the plants, i.e. besides seeds and leaves (Fig. 1a) also in pods and stems (not shown).

To induce senescence, detached leaves were incubated in permanent darkness (Fig. 1a). After 8d dark incubation, 84% of chl was retained in JI2775, thus showing a stronger retention than stay-green *Lolium temulentum* (Roca et al. 2004) or *Arabidopsis nye1* (Ren et al. 2007). Increase in the chl *a* to *b* ratio is a characteristic of senescence-related chl breakdown (Pružinská et al. 2005). This is caused by chl *b* to *a* reduction, which is a prerequisite of breakdown beyond the level of pheide (Scheumann et al. 1999). Consequently, the chl *a:b* ratio increased during dark-incubation of JI4 leaves, but not in JI2775, indicating that both chl *a* and *b* are retained to the same extend in the mutant (Fig. 1c).

Stay-greenness during senescence does not necessarily imply a conservation of photosynthetic capacity, as seen in other instances of non-functional or so called cosmetic stay-
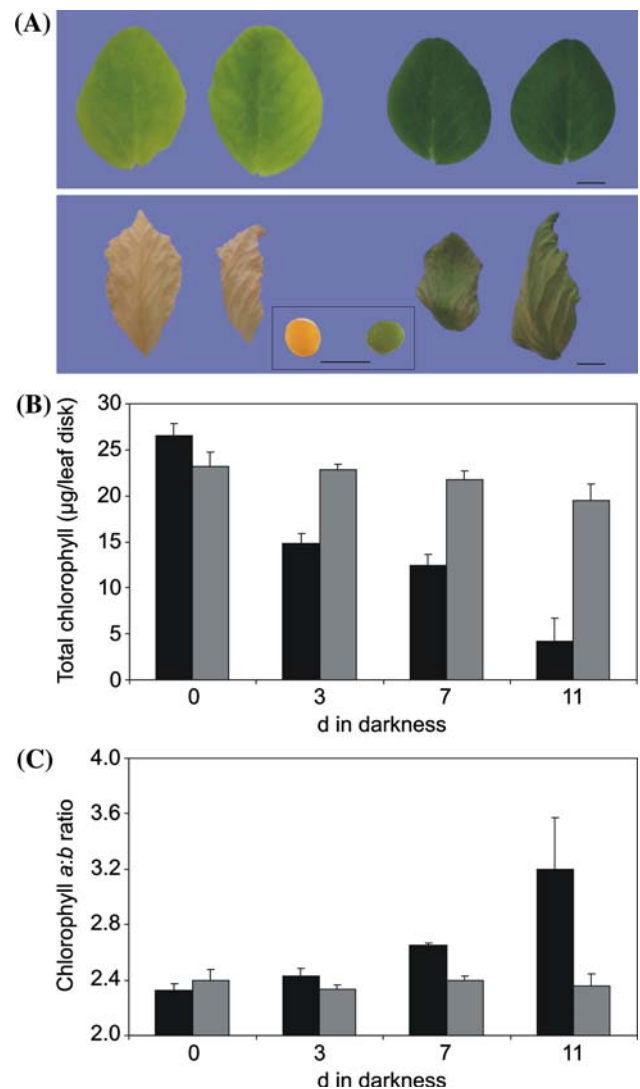
Fig. 1 Phenotype of the green cotyledon mutant JI2775 during chl breakdown. (**a**) Phenotype of individual leaves of JI4 (left) and JI2775 (right) after 11 days of dark-induced (upper panel) or natural senescence (lower panel). Inset, mature seeds from JI4 (left) and JI2775 (right) with the testa removed. Scale bars, 1 cm. (**b**) Degradation of chl in JI4 (black) and JI2775 (gray) during the course of dark-induced senescence. Data are means of a single representative experiment with three replicates. Error bars indicate SD. (**c**) Chl *a:b* ratio in JI4 (black) and JI2775 (gray) during the course of dark-induced senescence. Data are means of a single representative experiment with three replicates. Error bars indicate SD

greens (Kingston-Smith et al. 1997; Thomas and Howarth 2000). To examine the correlation between the greenness and leaf functionality, we covered attached pea leaves with aluminum foil in order to induce senescence and determined the maximal fluorescence yield (F_v/F_m) of photosystem II (PSII), reflecting the maximum quantum yield of the primary photochemistry of PSII (Fig. 2a). F_v/F_m decreased during the dark incubation in both lines, but the decrease was somewhat slower in JI2775 compared to JI4. We further analyzed F_0, an indicator of the connectivity of PSII

antenna with the core center (Havaux 1993; Oh et al. 2000). During leaf senescence, F_0 increased more drastically in JI4 (Fig. 2b), indicating dissociation of LHCII complexes from the PSII core. In contrast, in the mutant PSII integrity seemed to be retained much longer. Finally, the quantum yield of PSII electron transport (Φ_{PSII}) decreased slower in JI2775, but after 11 days had reached similar values like JI4 (Supplemental Fig. 1). Together, these fluorescence parameters indicated that senescence-related reduction of photosynthetic activity was somewhat slower in JI2775, but eventually reached levels comparable to the wild type. Moreover, the rate of net photosynthesis as determined by measuring net CO_2 fixation, decreased similarly during the course of senescence in both lines (Fig. 2c). Hence, photosynthetic activity was uncoupled from chl metabolism in the mutant, qualifying JI2775 a type C stay-green mutant according to a recently suggested nomenclature of stay-green mutants (Thomas and Howarth 2000).
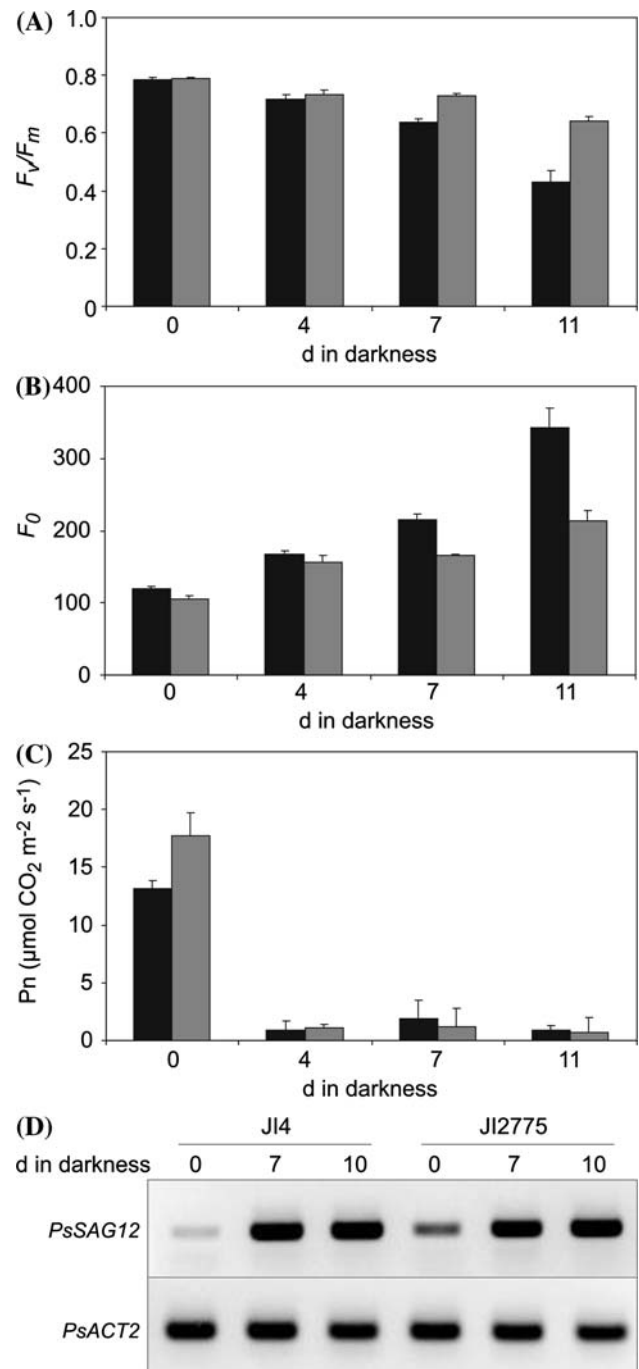
To further characterize the senescence behavior of JI2775, expression of *SAG12*, a commonly accepted marker of senescence (Quirino et al. 2000), was investigated by semiquantitative RT-PCR. In both lines, expression of *PsSAG12* increased to a similar extend during dark-induced senescence (Fig. 2d), indicating that senescence was initiated normally in the mutant.

We analyzed protein metabolism as a further marker of senescence progression. Again JI2775 behaved like JI4, i.e. overall protein degradation during dark-induced senescence was rather similar in both lines (data not shown). Nevertheless, differences were observed when individual photosynthesis-related proteins were analyzed by immunoblotting (Fig. 3a, b). LHCII was fully retained during the course of senescence in JI2775, a feature that has been described in different stay-green mutants (Hilditch et al. 1989; Bachmann et al. 1994; Pružinská et al. 2003; Park et al. 2007), but in contrast to the stay-green mutant Bf993 of *Festuca pratensis* (Thomas and Howarth 2000), proteolytic fragments of LHCII could not be detected in JI2775. In addition, core subunits of PSI (PsaD) and PSII (PsbA) were also retained to some extend in the mutant, and degradation of Rubisco subunits was somewhat slower in JI2775 compared to JI4. Together these data confirm earlier observations of high LHCII retention in stay-green mutants (Hilditch et al. 1989; Jiang et al. 2007; Park et al. 2007).

Overall, the diverse physiological data presented here confirm that JI2775 exhibits typical features of non-functional, type C stay-green mutants.

Isolation and characterization of *SGR* genes and proteins

By genomic mapping, SGR has been shown to locate to the *I* locus of Gregor Mendel's green cotyledon mutant

Fig. 2 Characterization of the senescence behavior of JI4 and JI2775. (a–c) Maximum quantum yield of PSII (F_v/F_m; a), minimum fluorescence in the dark (F_0; b) and net photosynthesis (Pn; c) during leaf senescence in JI4 (black) and JI2775 (gray). For senescence induction, attached leaves were covered with aluminum foil. Data are means of a single representative experiment with 6 replicates. Error bars indicate SE. (d) Semiquantitative analysis of expression of *PsSAG12* during senescence. *PsACT2* expression was used as control

(Armstead et al. 2007). This was recently indirectly confirmed by a segregation analysis exploiting the size differences of intron three of the pea *SGR* gene (Sato et al.
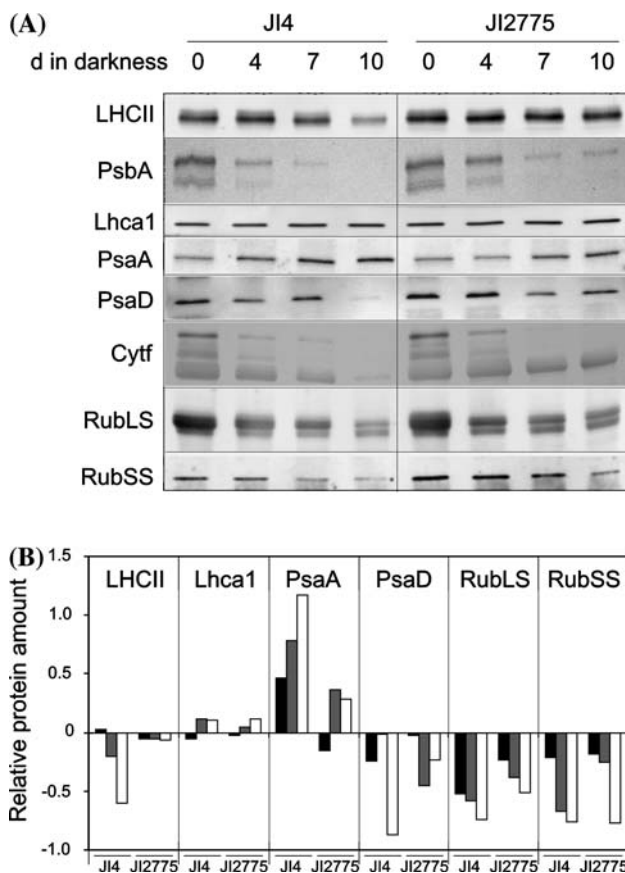
Fig. 3 Analysis of protein degradation during leaf senescence of JI4 and JI2775. (a) Immunoblot analysis of photosynthesis-related protein abundance in leaves of JI4 and JI2775 during dark-induced senescence. Antibodies against the following proteins were employed: LHCII and PsbA (photosystem II), LhcaI, PsaA and PsaD (photosystem I), Cytf (cytochrom b_6f complex) and Rubisco large (RubLS) and small subunit (RubSS). Gel loadings are based on equal amounts of fresh weight. (b) Relative changes of protein abundance as determined by quantifying the chemiluminescence signals of blots shown in (a). Bars represent relative changes of protein amounts after 4 days (black), 7 days (gray) and 10 days (white) of senescence as compared to 0 days samples. Thereby, negative values reflect degradation; positive values reflect increase of respective protein amounts. PsbA and Cytf blots (panel a) were visualized with a color substrate and, therefore, signals were not quantified

2007). We cloned the coding region of *PsSGR* from genomic DNA isolated from JI4 and JI2775. Thereby the genomic sequence was 81% and the coding sequence 99.8% identical between the two lines. Sequence differences were found at the same three positions of the coding region as described before (Sato et al. 2007), resulting in two missense mutations (Thr12Ser and Asn38Lys) and an Ile-Leu insertion after Ile189 of the deduced SGR protein of JI2775 as compared to JI4. Surprisingly, within the introns, sequence differences were limited to the third intron with an increase in size from 802 bases (JI4 SGR gene) to 923 bases in JI2775. Sequence identity of the third intron was 64%.

The completed *Arabidopsis* and rice genomes as well as additional available genomic sequences of SGRs were used to compare the exon/intron structure of SGR genes (Fig. 4a). The exact positions of introns were deduced by alignment of the genomic regions with expressed sequence tag (EST) sequences from respective species. The gene structure was conserved within the monocots and dicots, but differed from each other by the presence in the dicot genes of an additional intron splitting exon 2 of the monocot SGR genes (Fig. 3a). In all cases, introns were present at exactly the same positions within the coding regions indicating that SGR genes had existed prior to monocot and dicot divergence about 200 million years ago and that divergence is characterized by the occurrence of the additional intron. Consequently SGR-like genes are also found in lower plants, such as Gymnosperms (Ren et al. 2007), *Physcomitrella patens*, and eukaryotic algae, but also in some bacteria. The derived proteins cluster into several subclades, whereby monocot (clade I) and dicot SGR members (clade II) cluster together and are separated from lower species (Supplemental Fig. 2). Interestingly, a phylogenetically distant subclade of SGR homologues (clade III) contained further proteins from different higher plants, such as *Arabidopsis* and rice. In most cases of higher plant SGRs, expression of respective genes is supported by the presence of ESTs (not shown), but it remains to be demonstrated whether lower plant SGRs are functional orthologs of the higher plant proteins. An interesting feature of the monocot and dicot sequences in clade I and II, and of two *P. patens* sequences was the presence of a novel conserved motif near the C-terminal ends (Fig. 4b). The motif can be defined as Cys-X₃-Cys-X-Cys-Cys-Phe-Pro-X₇-Pro and is separated from the highly homologous core region of SGRs by a variable region of 12–38 amino acids in length. This motif was absent from the SGR-like proteins of clade III, and from lower plant and bacterial homologues. The presence of 4 conserved Cys residues implies possible functions in inter- or intramolecular crosslinking, or in redox regulation, but this has not yet been experimentally tested.

Interestingly, different isoforms are found in the (nearly) finished sequenced genomes of several species, such as *Arabidopsis thaliana*, *Vitis vinifera*, *Populus trichocarpa*, maize and rice. In *Arabidopsis* three *SGR* genes have been annotated, but a fourth gene, *AtSGR4*, is present as a tandem repeat of *AtSGR2* (At4g11910). This most likely represents a non-functional pseudogene, since ESTs cannot be identified in the available databases (data not shown). In order to identify the *SGR* gene number in pea, Southern blot analysis was performed with restricted genomic DNA of JI4 and JI2775 (Fig. 4c). The pattern of bands hybridizing with a *PsSGR* cDNA probe, indicate the presence in both pea lines of two *SGR* genes. This is confirmed by the
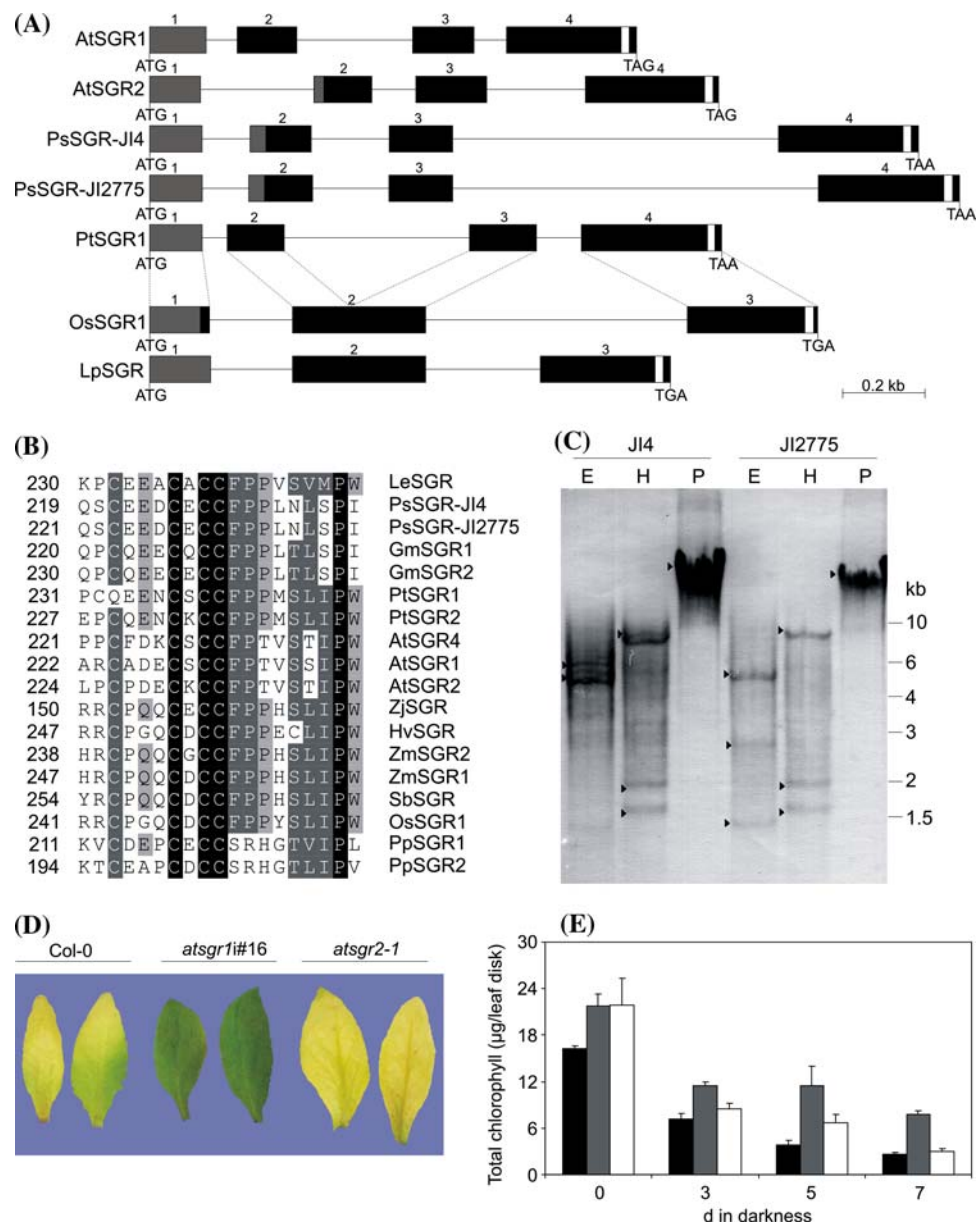
Fig. 4 SGR gene analyses, and analysis of *Arabidopsis* SGR-deficient lines. (a) Gene structure of dicotyledons and monocotyledons SGR genes with numbered exons (blocks) and introns (lines). Start and stop codons are shown. Predicted transit peptides (gray) and a conserved cystein-rich motif of unknown function (white; see also panel b) are shown. Intron/exon structures were determined by pair wise comparison of genomic and coding sequences. The accession numbers of sequences used in this analysis are as follows. Genomic sequences: *A. thaliana*, AtSGR1, NC_003075; AtSGR2, NC_003075; rice OsSGR, AP008215; pea PsSGR-JI4, AM884277; PsSGR-JI2775, AM884278; cDNA sequences: *A. thaliana*, AtSGR1, AY850161; AtSGR2, AY699948; OsSGR, AY850134; PsSGR-JI4, AB303331; PsSGR-JI2775, AB303332. *Populus trichocarpa* (PtSGR) sequences were obtained from the Joint Genome Institute (http://genome.jgi-psf.org/Poptr1_1/Poptr1_1.home.html; eugene3.00010981) *Lolium perenne* LpSGR sequences were provided by I.S. Donnison (personal communication). (b) Alignment of partial sequences from different plant SGRs identifies a novel conserved motif, which can be defined as $C-X_3-C-X-C_2FP-X_7-P$. Amino acid sequences were aligned using Dialign (http://bibiserv.techfak.uni-bielefeld.de/dialign). Black shading with white letters, gray shading with white letters, and gray shading with black letters reflect 100, 80, and 60% sequence conservation, respectively, with Blosum62 similarity groups enabled. For accession numbers of protein sequences, see Experimental procedures. (c) DNA gel blot analysis of *PsSGR*. 15 µg of genomic DNA from both JI4 and JI2775 were digested by *Eco*RI (E), *Hind*III (H) or *Pst*I (P) and probed with a digoxygenin-labeled *PsSGR* fragment from JI4. Arrowheads indicate cross-reacting bands. Sizes of DNA marker bands are indicated on the right. (d) Phenotype of leaves of Col-0, a *SGR1* silencing line (Armstead et al. 2007; *atsgr1*i#16) and a T-DNA insertion line of *AtSGR2* (*atsgr2-1*) after 5 days of dark-induced senescence. (e) Degradation of chl in Col-0 (black), *atsgr1*i#16 (gray) and *atsgr2-1* (white) during the course of detached leaf senescence. Data are means of a single representative experiment with 3 replicates. Error bars indicate SD.

Fig. 5 PsSGR mRNA and protein abundance, and PsSGR protein ▶ functionality test. (**a**) Semiquantitative analysis of *PsSGR* expression during leaf senescence in JI4 and JI2775. RNA abundance of *PsACT2* was used as control (**b**) Real-time RT-PCR quantification of *PsSGR* expression during senescence. Levels of expression were normalized to levels of *PsACT2* mRNA. Values are means of three replicates. (**c**) Immunoblot analysis of PsSGR protein levels during the course of detached leaf senescence. Gel loadings are based on equal amounts of fresh weight. (**d**) Transient expression of *PsSGR* in 3-week-old *N. benthamiana* plants. Leaves were infiltrated with *Agrobacterium tumefaciens* cultures containing plasmids for expression of PsSGR-JI2775 (JI2775), PsSGR-JI4 (JI4), or empty vector (Mock). Pictures show plants after 6 days of infiltration. (**e**, **f**) Analysis of leaf tissue after infiltration as in (**d**). (**e**) Total chl levels; (**f**) Immunoblot analysis of LHCII, PAO and SGR levels in the treatments. Gel loadings are based on equal sizes of leaf material. Control, non-infiltrated leaf tissue

presence in the databases of a pea EST (GenBank accession number AM162161), which is highly homologous, but not identical to *PsSGR*.

Two functional SGR genes have been identified in *Arabidopsis*, but so far only for the senescence-regulated *AtSGR1* (At4g22920) has an important function in chl breakdown been demonstrated (Armstead et al. 2007; Ren et al. 2007). In order to analyze whether *AtSGR2*, whose expression is also up-regulated during senescence (Park et al. 2007), is involved in chl catabolism as well, a homozygous T-DNA insertion line (SALK_003830C) was obtained from the SALK resource (Alonso et al. 2003). The line was termed *atsgr2-1* and position of the T-DNA within the first intron was confirmed by sequencing (Supplemental Fig. 3A). Expression of *AtSGR2* was absent (Supplemental Fig. 3B) indicating that *atsgr2-1* represents a null allele. During dark-induced senescence, chl was degraded at similar rates like in Col-0, in contrast to an *AtSGR* RNA silencing line (*atsgr1i#16*) (Armstead et al. 2007), which retained a large proportion of chl after 7 days of senescence (Fig. 4d, e). Although in *atsgr1i#16*, expression of *AtSGR2* was also slightly reduced (Supplemental Fig. 3B), silencing of *AtSGR1* expression in the knockout line *atsgr2-1* did not enhance the stay-green phenotype observed in *atsgr1i* (data not shown). This indicated that AtSGR2 does not significantly contribute to chl degradation in *Arabidopsis*. Likewise, the presence of two or more SGR gene copies in different species indicates either redundancy of SGR function in chl breakdown or implies that SGR might have additional role(s) in plant development that so far have escaped detection. Furthermore, the unclear role of the structurally similar SGR isoproteins of higher plants, such as AtSGR2, even more questions a function in chl breakdown of the less homologous SGR-like proteins from higher (clade III proteins) and lower plants (Supplemental Fig. 2). This has to be functionally tested, e.g. through complementation of the *nye1* mutant of *Arabidopsis*.
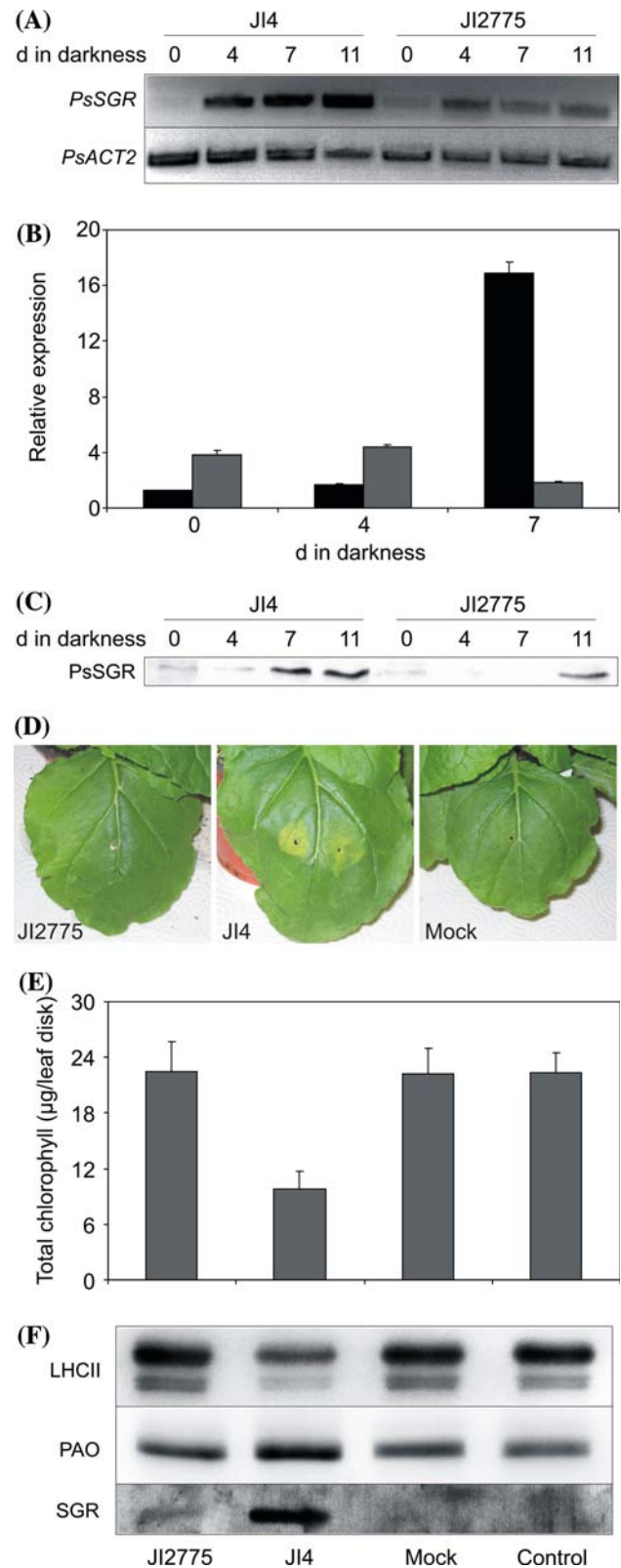
JI2775 is a loss-of-function mutant

In order to determine the molecular or biochemical defect of the pea mutant JI2775, we analyzed *PsSGR* gene

Fig. 6 Absence of SGR does not affect PAO abundance and activity. ▶
(a) Immunoblot analysis of PAO levels during the course of detached
leaf senescence in JI4 and JI2775. Gel loadings are based on equal
amounts of fresh weight. (b) Formation of pFCC-2 in PAO/RCCR
assays with PAO extracted from leaves of JI4 or JI2775 after 8 days
of dark-induced senescence. Activities are based on equal amounts of
fresh weight. HPLC traces (fluorescence at 320/450 nm) are shown.
Inset, Immunoblot analysis of PAO abundance in the extracts used for
PAO/RCCR assays. Gel loadings are based on equal amounts of fresh
weight. (c) Immunoblot analysis of PAO levels of individual AtSGR1-
silencing lines (atsgr1i; Armstead et al. 2007) after 5 days of dark-
induced senescence. Gel loadings are based on equal amounts of fresh
weight. (d) HPLC traces of leaf extracts from pea JI4 and JI2775, and
of a Lolium stay-green line (Lolium SG; Roca et al. 2004) after 8 and
5 days of dark-induced senescence, respectively, in the absence or
presence of 1 mM 2,2′ bipyridyl (BIP). Absorption of green-colored
chl catabolites was monitored at 665 nm. Analyzed extracts corre-
spond to equal amounts of fresh weight. Pigments were identified by
their absorption spectra and by comparison to authentic standards.
Pheide, standard containing both, pheide a and pheide b. The asterisk
marks a non-identified peak exhibiting a chl a spectrum

expression during leaf senescence by semiquantitative
(Fig. 5a) and real time RT-PCR (Fig. 5b). As shown earlier
for rice and Arabidopsis SGRs (Jiang et al. 2007; Park
et al. 2007; Ren et al. 2007), PsSGR expression was
strongly induced upon senescence induction of JI4. In
contrast, mRNA levels of JI2775 were kept on a lower
level during the course of senescence. This result was
obtained repeatedly in independent samples and confirmed
the low signals obtained in Northern blots from senescent
JI2775 leaves (Armstead et al. 2007). Sato et al. (2007)
reported that PsSGR gene expression was unaltered in
JI2775. To further analyze this discrepancy, SGR protein
levels were analyzed by immunoblotting using an antise-
rum directed against conserved motifs of SGR. In line with
our expression analysis, the senescence-related increase in
SGR protein observed in JI4 was significantly reduced in
the mutant (Fig. 5c). Together these data indicate that the
defect in JI2775 likely results from reduced expression of
PsSGR.

Nevertheless, the deduced protein sequence of SGR
from JI2775 exhibited changes compared to JI4-SGR, in
particular a two-amino acid insertion within a highly con-
served region that could affect SGR function. Therefore,
binary constructs were produced for both gene versions in
order to transform JI2775. Unfortunately, it was not pos-
sible to regenerate genetically transformed immature
embryos from JI2775 (A. Nadolska-Orczyk, personal
communication). Instead, we addressed this question by
heterologous transient expression in Nicotiana benthami-
ana leaves of SGR cDNA from either JI4 or JI2775. Five
days after infiltration, loss of chl was observed in the leaf
areas of plants that had been challenged with JI4-derived
SGR (Fig. 5d, e). In contrast, expression of SGR from
JI2775 did not induce chl breakdown in N. benthamiana
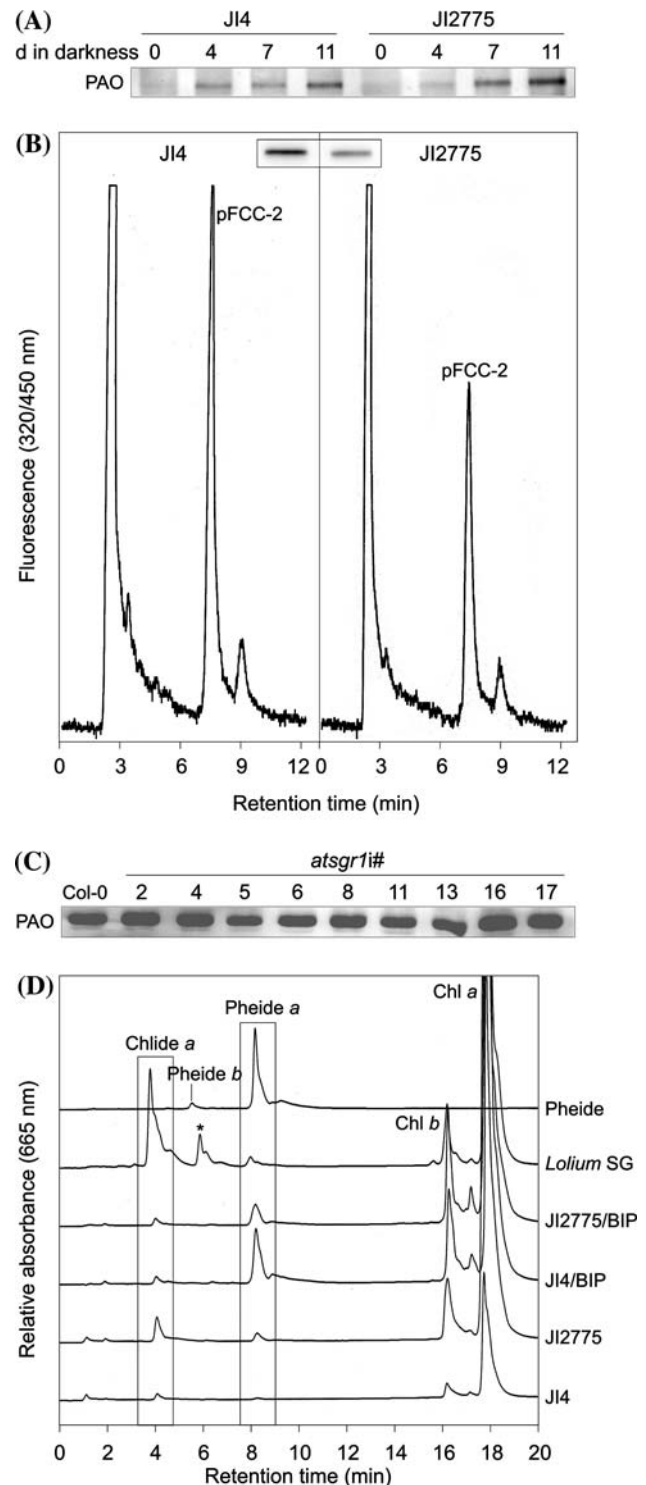
(Fig. 5d, e). Induction of senescence in the case of JI4-SGR
expression was confirmed by immunoblot analyses of total
protein extracts, which showed increased levels of PAO as
well as degradation of LHCII proteins (Fig. 5f). Although
SGR expression was comparable in both cases (data not
shown), much less protein accumulated in the case of
JI2775-SGR, compared to JI-SGR (Fig. 5f). This directly

demonstrated a loss of function of the mutated SGR, most likely caused by a loss of protein stability and, thus, confirms the indirect functional test performed by Sato et al. (2007). In conclusion, JI2775 is a loss-of-function mutant, which results from both reduced *SGR* gene expression and loss of SGR protein function.

SGR absence in JI2775 does not influence the PAO pathway

It had been proposed that the stay-green phenotype of the SGR/SID-deficient mutants Bf993 of *Festuca pratensis, nye1* of *Arabidopsis* and Mendel's green cotyledon mutant was caused by the (partial) loss of PAO function, which was in line with the observed accumulation during senescence of pheide *a* (Vicentini et al. 1995; Thomas et al. 1996; Roca et al. 2004; Ren et al. 2007). We re-addressed this assumption using JI4 and JI2775 and determining PAO abundance and activity. During 11 days of dark-induced senescence, PAO contents increased to comparable levels in both lines as judged by immunodetection (Fig. 6a). On the other hand, after extraction from senescent chloroplast membranes according to an established protocol (Hörtensteiner et al. 1995; Pružinská et al. 2005), PAO activity was 40% lower in extracts of JI2775 compared to the wild type (Fig. 6b). At first glance, this result indicated a posttranslational regulation of PAO, as has been proposed in canola seed development (Chung et al. 2006). In contrast, data on expression, protein abundance and activity suggest that PAO is transcriptionally regulated during *Arabidopsis* leaf senescence (Pružinská et al. 2005). When determining by immunoblotting the PAO content within the pea membrane extracts used for PAO assays, proportionally less PAO was found in the PAO extracts from the mutant (Fig. 6b, inset). This could be explained by the presence in senescent JI2775 leaves of large quantities of chloroplast membranes, which made a quantitative extraction of PAO impossible. We conclude that PAO abundance (and activity) are unchanged in the mutant compared to JI4. Likewise, PAO levels of senescent leaves were unaltered in different SGR-silencing lines of *Arabidopsis* (Fig. 6c). The same was true for a *Lolium* introgression line carrying the stay-green allele of *Festuca pratensis* Bf993 (H. Ougham, S. Hörtensteiner, I. Armstead, I. Donnison, I. King, H. Thomas and L. Mur, unpublished), although there lower PAO activities had been observed as well (Roca et al. 2004). Finally, Ren et al. (2007) also identified lower PAO activity in *nye1*, but unfortunately PAO protein abundance was not determined in this study. Altogether, the observed lower PAO activities in *sgr/sid* mutants (Fig. 6b; Vicentini et al. 1995; Roca et al. 2004; Ren et al. 2007) are due to misinterpretation of results and no indication remains of a

posttranslational regulation of PAO through SGR as suggested (Sato et al. 2007).

We also re-investigated the observation of pheide *a* accumulation in *sgr/sid* mutants. Pheide *a* did not accumulate in senescent JI4 leaves, but small quantities (5–10 nmol pheide *a* g^{-1} fresh weight) were found in JI2775 (Fig. 6d). If the occurrence in JI4 of pheide *a* would solely be the result of partial inhibition of PAO in an otherwise normally active chl breakdown pathway, it could be expected that entire inhibition of PAO would increase the amount of pheide *a*. To analyze this, leaves were senesced in the presence of 2,2′-bipyridyl, an iron chelator, which among other reactions has been shown to inhibit PAO (Hörtensteiner et al. 1995; Hörtensteiner et al. 2000). In wild type, bipyridyl-treatment largely enhanced the accumulation of pheide *a* (80 nmol g^{-1} fresh weight), but this increase was much smaller in JI2775 (35 nmol g^{-1} fresh weight). These data indicate that occurrence of pheide *a* is independent of PAO. Instead, pheide *a* formation could result from non-physiological conversion from chlide *a*. This might be due to tissue acidification as a consequence of tonoplast rupture upon cell damage or death occurring at later stages of leaf senescence. Chlide *a* repeatedly accumulated to higher concentrations in senescent leaves of the mutant compared to JI4 (Fig. 6d), an observation that had been made also in other instances of *sgr/sid* mutants (Vicentini et al. 1995; Roca et al. 2004). Particularly in Bf993 and the stay-green introgression lines of *Lolium*, large quantities accumulated in senescent leaves. This intriguing observation correlates to the fact that, compared to rice and pea *sgr* mutants, the *Festuca/Lolium sid* lines are null mutants, caused by a frame shift mutation within the second exon of the gene (Armstead et al. 2006). In this respect it is possible to argue that SGR/SID might affect Mg-dechelation. This step in chl breakdown was shown to be catalyzed nonenzymatically by a heat-stable, low molecular weight compound, termed metal chelating substance. Metal-chelating substances of different species have different molecular weights, but their structures have so far not been elucidated (Costa et al. 2002; Suzuki et al. 2005). Alternatively, metal-chelating substance might represent the metal-chelating cofactor of a Mg-dechelatase enzyme (Hörtensteiner 2006) and it remains to be investigated whether SGR could have this function.

Altogether the data presented here refute the suggestion of several groups of impairment of PAO function in SGR mutants, hence, most likely the biochemical steps of the PAO pathway of chl breakdown are not regulated by SGR.

SGR acts upstream of PAO

If SGR does not regulate the biochemical enzymes of chl breakdown, at which level does it then interfere with chl
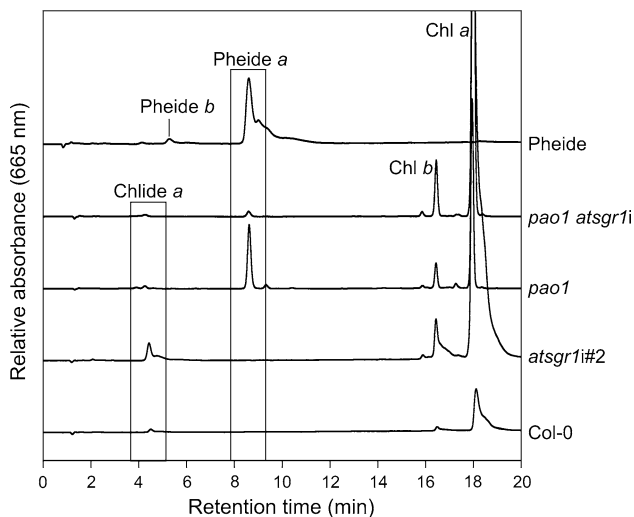
Fig. 7 HPLC analysis of green chl catabolites in *SGR1*- and *PAO*-deficient *Arabidopsis*. Equal amounts of leaf extracts from Col-0, *atsgr1*i#2 (Armstead et al. 2007), *pao1* (Pružinská et al. 2005) and a representative line silencing *AtSGR1* in *pao1* background (*pao1 atsgr1*i) were separated by reversed-phase HPLC, and A_{665} was monitored. Pigments were identified by their absorption spectra and by comparison to authentic standards. Pheide, standard containing both, pheide *a* and pheide *b*

metabolism? In order to address this question, we silenced expression of *AtSGR1* in the *pao1* background (Pružinská et al. 2005). Two independent homozygous lines, *pao1 atsgr1*i#1 and *pao1 atsgr1*i#2, were isolated and further analyzed. During senescence, the lines exhibited a stay-green phenotype, but a cell death phenotype, typical for *pao1*, did not establish in the *pao1 atsgr1*i lines (data not shown). Furthermore, in contrast to *pao1*, pheide *a* accumulation was largely reduced in the *pao1 atsgr1*i lines (Fig. 7). This result indicated that abolishment of SGR function prevents pheide *a* formation, hence confirms that the SGR target is located upstream of PAO.

Conclusion

The identification and analysis of the role of SGR/SID proteins during plant senescence has recently become a major focus in plant senescence research. This is demonstrated by the high number of reports about identification of *sgr/sid* mutants and the recent cloning of *SGR/SID* genes from *Arabidopsis*, *Festuca/Lolium*, pea and rice (Armstead et al. 2006, 2007; Jiang et al. 2007; Park et al. 2007; Ren et al. 2007; Sato et al. 2007). It is likely that additional stay-green mutants, such as tomato *green flesh* (*gf*; Akhtar et al. 1999) and pepper *chlorophyll retainer* (*cl*; Efrati et al. 2005) are defective in *SGR* as well. Only some of these mutants have been attributed to the class of type C

non-functional stay-greens. Here we show that Gregor Mendel's *I* mutant also belongs to this class.

Analysis of the different *sgr/sid* mutants available so far, indicate that overall reduction of SGR gene expression (Armstead et al. 2007) or loss of function due to mutations within the open reading frames of SGR genes (Jiang et al. 2007; Park et al. 2007; Ren et al. 2007) can cause the stay-green phenotype. In this respect, Mendel's *I* mutant is exceptional, since we here show that both gene expression and protein function are affected. An explanation for the reduced mRNA level most probably is an altered SGR promoter activity in the mutants, but this remains to be confirmed.

SGR/SID proteins constitute a new class of senescence proteins, which are widely distributed in plants. The absence of known domains makes it impossible to deduce a function from the primary sequence of SGR proteins. Conflicting reports in the literature indicated an activity of SGR in relation to either PAO function and/or chl-apoprotein dismantling (Vicentini et al. 1995; Thomas et al. 1996; Roca et al. 2004; Park et al. 2007; Ren et al. 2007). With the results presented here, we unambiguously demonstrate that SGR does not regulate PAO. We furthermore show that SGR functions upstream of PAO, but the exact site of action remains to be elucidated. Park et al. (2007) showed physical interaction between SGR and LHCII subunits and suggested that SGR might be required for dismantling of chl-apoprotein complexes. In this case SGR would *senso stricto* not be part of the catabolic machinery of chl breakdown directly, but its action would be a prerequisite for allowing the catabolic enzymes to get access to their substrate. An interesting observation is that in *pao1* SGR gene expression is not up-regulated during senescence (Park et al. 2007). It is likely that this regulation is achieved through pheide *a*, although, in contrast to the suggested retrograde signaling by porphyrin intermediates of chl biosynthesis (Nott et al. 2006), pheide *a* most probably is not a retrograde signal itself. Nevertheless, the proposed function in the dismantling of chl-protein complexes (Park et al. 2007) provides an ideal point of control of chl breakdown. In addition, the retention of chl-binding proteins suggests that proteases known to degrade LHC proteins during senescence, such as FtsH6 (Zelisko et al. 2005), are either directly regulated through SGR or complex-dismantling is also a prerequisite for the respective proteases to get access to their substrate proteins. In this respect, the analysis of the rice *nyc1* mutant provides an interesting alternative (Kusaba et al. 2007); chl *b* is known to be required in a certain stoichiometry to chl *a* in order to stabilize chl-protein complexes (Horn and Paulsen 2004), thus, prevention of chl *b* to chl *a* conversion in *nyc1* would stabilize the complexes. It will be interesting to analyze the regulation of SGR in *nyc1* and to

see whether NYC1 or SGR or both regulate chl-protein complex stability.

References

Akhtar MS, Goldschmidt EE, John I, Rodoni S, Matile P, Grierson D (1999) Altered patterns of senescence and ripening in *gf*, a stay-green mutant of tomato (*Lycopersicon esculentum* Mill.). J Exp Bot 50:1115–1122

Alonso JM, Stepanova AN, Leisse TJ, Kim CJ, Chen H, Shinn P, Stevenson DK, Zimmermann J, Barajas P, Cheuk R, Gadrinab C, Heller C, Jeske A, Koesema E, Meyers CC, Parker H, Prednis L, Ansari Y, Chory N, Deen H, Geralt M, Hazari N, Hom E, Karnes M, Mulholland C, Ndubaku R, Schmidt I, Guzman P, Aguilar-Henonin L, Schmid M, Weigel D, Carter DE, Marchand T, Risseeuw E, Brogden D, Zeko A, Crosby WL, Berry CC, Ecker JR (2003) Genome-wide insertional mutagenesis of *Arabidopsis thaliana*. Science 301:653–657

Armstead I, Donnison I, Aubry S, Harper J, Hörtensteiner S, James C, Mani J, Moffet M, Ougham H, Roberts L, Thomas A, Weeden N, Thomas H, King I (2006) From crop to model to crop: identifying the genetic basis of the staygreen mutation in the *Lolium/Festuca* forage and amenity grasses. New Phytol 172:592–597

Armstead I, Donnison I, Aubry S, Harper J, Hörtensteiner S, James C, Mani J, Moffet M, Ougham H, Roberts L, Thomas A, Weeden N, Thomas H, King I (2007) Cross-species identification of Mendel's *I* locus. Science 315:73

Bachmann A, Fernández-López J, Ginsburg S, Thomas H, Bouwcamp JC, Solomos T, Matile P (1994) *Stay-green* genotypes of *Phaseolus vulgaris* L.: chloroplast proteins and chlorophyll catabolites during foliar senescence. New Phytol 126:593–600

Bhattacharyya MK, Smith AM, Ellis THN, Hedley C, Martin C (1990) The wrinkled-seed character of pea described by Mendel is caused by a transposon-like insertion in a gene encoding starch-branching enzyme. Cell 60:115–122

Chakraborti D, Sarkar A, Gupta S, Das S (2006) Small and large scale genomic DNA isolation protocol for chickpea (*Cicer arietinum* L.), suitable for molecular marker and transgenic analyses. Afr J Biotechnol 5:585–589

Chung DW, Pružinská A, Hörtensteiner S, Ort DR (2006) The role of pheophorbide *a* oxygenase expression and activity in the canola green seed problem. Plant Physiol 142:88–97

Costa ML, Civello PM, Chaves AR, Martinez GA (2002) Characterization of Mg-dechelatase activity obtained from *Fragaria × ananassa* fruit. Plant Physiol Biochem 40:111–118

Efrati A, Eyal Y, Paran I (2005) Molecular mapping of the *chlorophyll retainer* (*cl*) mutation in pepper (*Capsicum* spp.) and screening for candidate genes using tomato ESTs homologous to structural genes of the chlorophyll catabolism pathway. Genome 48:347–351

Gray J, Wardzala E, Yang M, Reinbothe S, Haller S, Pauli F (2004) A small family of LLS1-related non-heme oxygenases in plants with an origin amongst oxygenic photosynthesizers. Plant Mol Biol 54:39–54

Havaux M (1993) Characterization of thermal damage to the photosynthetic electron transport system in potato leaves. Plant Sci 94:19–33

Hellens R, Edwards EA, Leyland NR, Bean S, Mullineaux PM (2000) pGreen: a versatile and flexible binary Ti vector for *Agrobacterium*-mediated plant transformation. Plant Mol Biol 42:819–832

Hilditch P, Thomas H, Rogers L (1986) Leaf senescence in a non-yellowing mutant of *Festuca pratensis*: Photosynthesis and photosynthetic electron transport. Planta 167:146–151

Hilditch PI, Thomas H, Thomas BJ, Rogers LJ (1989) Leaf senescence in a non-yellowing mutant of *Festuca pratensis*: proteins of photosystem II. Planta 177:265–272

Horn R, Paulsen H (2004) Early steps in the assembly of light-harvesting chlorophyll *a/b* complex - Time-resolved fluorescence measurements. J Biol Chem 279:44400–44406

Hörtensteiner S (2006) Chlorophyll degradation during senescence. Annu Rev Plant Biol 57:55–77

Hörtensteiner S, Vicentini F, Matile P (1995) Chlorophyll breakdown in senescent cotyledons of rape, *Brassica napus* L.: enzymatic cleavage of phaeophorbide *a in vitro*. New Phytol 129:237–246

Hörtensteiner S, Chinner J, Matile P, Thomas H, Donnison IS (2000) Chlorophyll breakdown in *Chlorella protothecoides*: characterization of degreening and cloning of degreening-related genes. Plant Mol Biol 42:439–450

Jiang H, Li M, Liang N, Yan H, Wei Y, Xu X, Liu J, Xu Z, Chen F, Wu G (2007) Molecular cloning and function analysis of the *stay green* gene in rice. Plant J 52:197–209

Kingston-Smith AH, Thomas H, Foyer CH (1997) Chlorophyll *a* fluorescence, enzyme and antioxidant analyses provide evidence for the operation of alternative electron sinks during leaf senescence in a *stay-green* mutant of *Festuca pratensis*. Plant Cell Environ 20:1323–1337

Kreuz K, Tommasini R, Martinoia E (1996) Old enzymes for a new job. Herbicide detoxification in plants. Plant Physiol 111:349–353

Kürsteiner O, Dupuis I, Kuhlemeier C (2003) The *pyruvate decarboxylase1* gene of Arabidopsis is required during anoxia but not other environmental stresses. Plant Physiol 132:968–978

Kusaba M, Ito H, Morita R, Iida S, Sato Y, Fujimoto M, Kawasaki S, Tanaka R, Hirochika H, Nishimura M, Tanaka A (2007) Rice NON-YELLOW COLORING1 is involved in light-harvesting complex II and grana degradation during leaf senescence. Plant Cell 19:1362–1375

Lester DR, Ross JJ, Davies PJ, Reid JB (1997) Mendel's stem length gene (*Le*) encodes a gibberellin 3β-hydroxylase. Plant Cell 9:1435–1443

Llave C, Kasschau KD, Carrington JC (2000) Virus-encoded suppressor of posttranscriptional gene silencing targets a maintenance step in the silencing pathway. Proc Natl Acad Sci USA 97:13401–13406

Matile P, Hörtensteiner S, Thomas H (1999) Chlorophyll degradation. Annu Rev Plant Physiol Plant Mol Biol 50:67–95

Maxwell K, Johnson GN (2000) Chlorophyll fluorescence—a practical guide. J Exp Bot 51:659–668

Mendel G (1866) Versuche über Pflanzenhybriden. Verh Naturforsch Ver Brünn 4:3–47

Müller T, Moser S, Ongania K-H, Pružinská A, Hörtensteiner S, Kräutler B (2006) A divergent path of chlorophyll breakdown in the model plant *Arabidopsis thaliana*. ChemBioChem 7:40–42

Murray MG, Thompson WF (1980) Rapid isolation of high molecular-weight plant DNA. Nucl Acids Res 8:4321–4325

Nott A, Jung HS, Koussevitzky S, Chory J (2006) Plastid-to-nucleus retrograde signaling. Annu Rev Plant Biol 57:739–759

Oberhuber M, Berghold J, Breuker K, Hörtensteiner S, Kräutler B (2003) Breakdown of chlorophyll: a nonenzymatic reaction accounts for the formation of the colorless "nonfluorescent" chlorophyll catabolites. Proc Natl Acad Sci USA 100:6910–6915

Oh MH, Kim YJ, Lee CH (2000) Leaf senescence in a stay-green mutant of *Arabidopsis thaliana*: disassembly process of photosystem I and II during dark-incubation. J Biochem Mol Biol 33:256–262

Park S-Y, Yu J-W, Park J-S, Li J, Yoo S-C, Lee N-Y, Lee S-K, Jeong S-W, Seo HS, Koh H-J, Jeon J-S, Park Y-I, Paek N-C (2007) The senescence-induced staygreen protein regulates chlorophyll degradation. Plant Cell 19:1649–1664

Pružinská A, Anders I, Tanner G, Roca M, Hörtensteiner S (2003) Chlorophyll breakdown: pheophorbide *a* oxygenase is a Rieske-type iron-sulfur protein, encoded by the *accelerated cell death 1* gene. Proc Natl Acad Sci USA 100:15259–15264

Pružinská A, Tanner G, Aubry S, Anders I, Moser S, Müller T, Ongania K-H, Kräutler B, Youn J-Y, Liljegren SJ, Hörtensteiner S (2005) Chlorophyll breakdown in senescent Arabidopsis leaves: characterization of chlorophyll catabolites and of chlorophyll catabolic enzymes involved in the degreening reaction. Plant Physiol 139:52–63

Pružinská A, Anders I, Aubry S, Schenk N, Tapernoux-Lüthi E, Müller T, Kräutler B, Hörtensteiner S (2007) In vivo participation of red chlorophyll catabolite reductase in chlorophyll breakdown. Plant Cell 19:369–387

Quirino BF, Noh YS, Himelblau E, Amasino RM (2000) Molecular aspects of leaf senescence. Trends Plant Sci 5:278–282

Ren G, An K, Liao Y, Zhou X, Cao Y, Zhao H, Ge X, Kuai B (2007) Identification of a novel chloroplast protein AtNYE1 regulating chlorophyll degradation during leaf senescence in Arabidopsis. Plant Physiol 144:1429–1441

Roca M, James J, Pružinská A, Hörtensteiner S, Thomas H, Ougham H (2004) Analysis of the chlorophyll catabolism pathway in leaves of an introgression senescence mutant of *Lolium temulentum*. Phytochemistry 65:1231–1238

Sato Y, Morita R, Nishimura M, Yamaguchi H, Kusaba M (2007) Mendel's green cotyledon gene encodes a positive regulator of the chlorophyll-degrading pathway. Proc Natl Acad Sci USA 104:14169–14174

Scheumann V, Schoch S, Rüdiger W (1999) Chlorophyll *b* reduction during senescence of barley seedlings. Planta 209:364–370

Sidler M, Hassa P, Hasan S, Ringli C, Dudler R (1998) Involvement of an ABC transporter in a developmental pathway regulating hypocotyl cell elongation in the light. Plant Cell 10:1623–1636

Strain HH, Cope BT, Svec WA (1971) Analytical procedures for the isolation, identification, estimation and investigation of the chlorophylls. Methods Enzymol 23:452–476

Suzuki T, Kunieda T, Murai F, Morioka S, Shioi Y (2005) Mg-dechelation activity in radish cotyledons with artificial and native substrates, Mg-chlorophyllin *a* and chlorophyllide *a*. Plant Physiol Biochem 43:459–464

Thomas H (1987) *Sid*: a Mendelian locus controlling thylakoid membrane disassembly in senescing leaves of *Festuca pratensis*. Theor Appl Genet 73:551–555

Thomas H (1997) Chlorophyll: a symptom and a regulator of plastid development. New Phytol 136:163–181

Thomas H, Howarth CJ (2000) Five ways to stay green. J Exp Bot 51:329–337

Thomas H, Schellenberg M, Vicentini F, Matile P (1996) Gregor Mendel's green and yellow pea seeds. Bot Acta 109:3–4

Vicentini F, Hörtensteiner S, Schellenberg M, Thomas H, Matile P (1995) Chlorophyll breakdown in senescent leaves: identification of the biochemical lesion in a *stay-green* genotype of *Festuca pratensis* Huds. New Phytol 129:247–252

Wesley SV, Helliwell CA, Smith NA, Wang M, Rouse DT, Liu Q, Gooding PS, Singh SP, Abbot D, Stoutjesdijk PA, Robinson SP, Gleave AP, Green AG, Waterhouse PM (2001) Construct design for efficient, effective and high-throuput gene silencing in plants. Plant J 27:581–590

White OE (1916) Inheritance studies in *Pisum* I Inheritance of cotyledon color. Am Nat 50:530–547

Zelisko A, Garcia-Lorenzo M, Jackowski G, Jansson S, Funk C (2005) AtFtsH6 is involved in the degradation of the light-harvesting complex II during high-light acclimation and senescence. Proc Natl Acad Sci USA 102:13699–13704